DE GRUYTER Open Chem., 2018; 16: 605–613

Research Article Open Access

Vivek Srivastava*

# Synthesis and Characterization of Pd exchanged MMT Clay for Mizoroki-Heck Reaction

https://doi.org/10.1515/chem-2018-0065
received February 26, 2018; accepted April 24, 2018.

**Abstract:** We successfully synthesized Pd@MMT clay using a cation exchange process. We characterized all the synthesized Pd@MMT clays using sophisticated analytical techniques before testing them as a heterogeneous catalyst for the Mizoroki - Heck reaction (mono and double). The highest yield of the Mizoroki-Heck reaction product was recovered using thermally stable and highly reactive Pd@MMT-1 clay catalyst in the functionalized ionic liquid reaction medium. We successfully isolated 2-aryl-vinyl phosphonates (mono-Mizoroki-Heck reaction product) and 2,2-diaryl-vinylphosphonates (double-Mizoroki-Heck reaction product) using aryl halides and dialkyl vinyl phosphonates in higher yields. The low catalyst loading, easy recovery of reaction product and 8 times catalyst recycling are the major highlights of this proposed protocol.

**Keywords:** Mizoroki-Heck reaction; MMT clay; Palladium; C-C coupling; Ionic liquids; Nanoparticles.

## 1 Introduction

Palladium metal is considered one of the most well-investigated materials among the series of transition metals for C-C coupling reactions [1-3]. Several forms of palladium metal, such as Pd metal complex with carbenesand phosphines as well as palladium salts have been utilized as a catalyst [3-5]. Palladium metal was also supported on different organic and inorganic supports to make the Pd metal catalyst more active and stable in terms of air and moisture issues, substrate scope, catalyst leaching and catalyst loading. Recently, different synthetic protocols have been introduced to synthesize Pd nanoparticles (NPs) which utilize the advanced Physio-chemical properties of nanoparticles such as high degree of dispersion in reaction mass and the large surface area [4-8] when applying Pd NPs as nanocatalysts for different organic transformations. In some of the reports, the extraordinary nature of these Pd NPs has been recorded for different types of C-C coupling reactions like Suzuki, Mizoroki-Heck and Sonogashira reaction [6-8]. Although, Pd NPs appeared as an important form of Pd catalyst, unfortunately, they also suffer with some unique problems of nanoparticles like stability, agglomeration and uneven size distribution of Pd NPs during the chemical reaction. In some of the scientific reports, Pd NPs were supported on different organic/inorganic supports like polymer, ionic liquid, activated carbon, silica, MCM-41, clays. $Al_2O_3$ and Zeolite get agglomeration free and stable Pd NPs, but the curse of a costly starting material, tedious synthetic protocol and, most important, reproducibility of synthetic protocol collectively hurts the supported synthesis of Pd NPs [8-12].

Na-Montmorillonite clay (MMT) is one of the important materials which is used as a support for various transition metals, mainly because of its exceptional physiochemical properties such as high cation exchange capacity and good swelling properties [13]. Additionally, MMT supported catalytic systems also offer, a high degree of thermal stability, provides protection to metal against air/moisture, easy catalyst isolation and recycling. The interlayer spacing of aluminosilicates in MMT is filled with several $Na^+$, $K^+$ and $Ca^{2+}$ ions, these ions are considered as exchangeable cations in MMT, which are mainly responsible for the metal ion exchange reaction [13-15]. MMT supported metal has been tested as a catalyst for several reactions like oxidation, reduction, transesterification and coupling reactions, but to achieve maximum metal exchange as well as high catalyst loading are still a challenge [13-18].

Ionic liquids (ILs) are organic salts that are liquid below 100°C and have received considerable attention as substitutes for volatile organic solvents. Since they are nonflammable, non-volatile and recyclable, they are classified as green solvents. Due to their amazing properties, such as outstanding solvating potential,

---

***Corresponding author: Vivek Srivastava,** NIIT University, NH-8 Jaipur/Delhi Highway, Neemrana, Rajasthan, Pin Code: 301705, India, E-mail: vivek.shrivastava@niituniversity.in

thermal stability and their tunable properties by suitable choices of cations and anions, they are considered as a favorable reaction medium over conventional solvent systems for chemical synthesis [4]. ILs are mainly made up of cationic and anionic components that can be arranged to achieve a specific set of properties. In this context, the term “designer solvents” has been used to illustrate the potential of this environment-benign ILs in chemical transformations. Being designer solvents, they can be modified as per the specific requirement of the reaction conditions, therefore they also name as “task specific ILs (TSILs).” Since these liquids, can dissolve a series of transition metal complexes, they have been utilized as an alternative for conventional solvent systems in many transition metal complex catalyzed organic transformations to get enhanced reaction rates, selectivity and catalyst recycling with easy isolation of the reaction product [13-20]. The present study is aimed to explore the application of ionic liquid as TSIL to avoid the use of a toxic base in the Mizoroki - Heck reaction.

In this paper, we are presenting the controlled synthesis of Pd NPs within the interlayer spacing of MMT followed by cation exchange method, where Pd metal (using tetraamminepalladium(II) chloride monohydrate as substrate) ions were exchanged by interlayer cations ($Na^+$, $K^+$ or $Ca^{2+}$) of MMT. We utilized Pd@MMT clay as a catalyst for the Mizoroki - Heck reaction in TSILs (1,3-*di*(*N*, *N*-dimethylaminoethyl)-2-methylimidazolium *bis* (trifluoromethylsulfonyl) imide ([DAMI][$NTf_2$])) to synthesize 2-aryl and 2,2-diary vinylphohonates. It is well documented that ionic liquid interacts very effectively with transition metal catalysts. In addition, we will also investigate the Pd@ MMT/ionic liquid recycling test. High reaction rate, base free reaction process, stable nano-catalytic system, low catalyst loading, easy product isolation and catalyst recycling are the most interesting features of this proposed protocol.

## 2 Experimental

All the reagent grade chemicals were purchased from Sigma Aldrich and SD Fine chemicals. All the $^1H$ and $^{13}C$ NMR spectra were recorded with 400 MHz Bruker spectrometer with the $CDCl_3$ solvent system. The internal standard for $^1H$ and $^{13}C$ NMR spectra were kept at 7.26 and 7.36 ppm respectively (supporting information). $^{31}P$ NMR spectra of all the unknown compounds were recorded Varian 400 NMR spectrometer (85% $H_3PO_4$ as an external standard) (supporting information). The Na MMT was supplied from Southern Clay Product, Texas-USA with the registered product name Cloisiite Na and it was used for tetraamminepalladium(II) chloride monohydrate intercalation without going to any further purification of pretreatment process. The cation exchange capacity (CEC) of Na-montmorillonite was 92.6 mequiv/100 g [13-15]. Philips X’Pert MPD instruments were used to record all small and wide-angle X-Ray Powder Diffraction (XRD) data using an X-ray tube voltage of 30.0 kV and current of 15.0 mA, scan rate of 5/min and step size of 0.05. The fine powder of Pd@MMT clay was mixed with vacuum grease and fixed on the glass substrate. A flat surface was obtained by pressing the mixed powder between two flat glass sheets. The diffraction pattern was obtained after subtraction of the powder spectrum from the background of a glass substrate plus the vacuum grease.

The Pd@MMT clay material was characterized by TEM (Hitachi S-3700N). The TEM sample was prepared by mixing the Pd@MMT sample with epoxy resin distributed between two silicon wafer pieces at $50^oC$ for 30 minutes. Cross section of TEM samples were pre-thinned mechanically followed by ion milling. Particle size distribution was determined once the original negative had been digitalized and expanded to 500 pixels per cm for more accurate resolution and measurement.

EDX spectra were measured with a Si(Li) EDS detector (Thermo Scientific) or an XFlash® SDD detector (Bruker), both having an active area of 10 $mm^2$. A large-area SDD EDS detector (Bruker) capable of high-sensitivity detection has been used for some specific samples.

The specific surface area (BET) of the catalyst was determined on a Micrometrics Flowsorb III 2310 instrument. The samples were dried with nitrogen purging or in a vacuum applying elevated temperatures. We used $P/P_0$ of 0,1, 0,2 and 0,3 as standard measurement points. The volume of gas adsorbed to the surface of the particles is measured at the boiling point of nitrogen (-196°C). The amount of adsorbed gas is correlated to the total surface area of the particles including pores in the surface. The calculation is based on the BET theory. Traditionally nitrogen is used as adsorbate gas. Gas adsorption also enables the determination of size and volume distribution of micropores (0.35 – 2.0 nm).

Fourier transform infrared spectrophotometer (FTIR) analysis of all the samples were studied with Bruker Tensor-27. Elemental analysis was conducted in a Perkin Elmer Optima 3300 XL. All the solid samples were prepared by using KBr pellets while liquid samples were prepared by using nujol as an internal reference.

ICP-OES (inductively coupled plasma atomic emission spectroscopy) was applied to determine the metal Pd and phosphorus content. A sample for ICP-OES analysis was prepared by accurately weighing 2.00 g of Pd@MMT and placing in a pre-cleaned 100 mL volumetric flask. An optimized amount of extractant solution (10 mL Aqua Regia) was then added and the resulting mixture irradiated at the optimum sonication time of 120 min to guarantee maximum sample irradiation, and the volumetric flasks were kept stationary at selected positions in the bath with only four samples used for simultaneous sonication. The resulting supernatant liquid was separated from the solid phase by centrifugation at 2500 rpm for 15 min, after which diluted up to 40.0 g with Milli-Q water before going to ICP-OES analysis.

1,3-*di* (*N*, *N*-dimethylaminoethyl) -2-methylimidazolium *bis* (trifluoromethylsulfonyl) imide ([DAMI] [$NTf_2$]) and 1-butyl-3-methylimidazolium bis (trifluoromethylsulfonyl) imide ([Bmim] [$NTf_2$]) were synthesized as per reported procedure [4 and 17].

## 2.1 Synthesis of Pd@MMT Clay

A perfectly cleaned and dried 250 mL round bottom flask was charged with the suspension of Na MMT clay (5 g) with 100 mL water. The aqueous solution of 50 mL of tetraamminepalladium (II) chloride monohydrate (6 mM) solution was added in dropwise manner into the homogeneous slurry of Na MMT clay within 2 hours by maintaining the pH of the solution at 5.5 (using 0.1N HCl). The combined reaction was stirred at 25-30°C for the next 24 hours to obtain a uniform dispersion. Later, $[Pd(NH_3)_4]$ -MMT exchanged clay was stirred with $NaBH_4$ (5 g) for the next 5 hours at room temperature. The color change from brown to black confirmed the complete reduction of $Pd^{2+}$ to $Pd^0$. Further, Pd exchanged clay was washed with double distilled water using centrifugation. Washing was stopped as soon as we got chloride free supernatant (monitored with silver nitrate solution). Finally, chloride free Pd exchanged clay was dried under lyophilizer for 12 hours. At last, we obtained free-flowing black colored powder as Pd@MMT-1 clay (4.8 g, 3w/w % Pd). In the same pattern, we also prepared Pd@MMT-2 clay (4.3 g, 1.01 w/w % Pd) using tetraamminepalladium(II) chloride monohydrate solution (3 mM) with 5 g Na MMT clay. pH of the above-mentioned reaction mass was also controlled by the addition 0.1 N HCl.

## 2.2 Experimental Procedure of Mono or Double Mizoroki-Heck Reaction

50 mL glass-made reaction vessel was charged with aryl halides and vinylphosphonate with Pd@MMT clay -1 or 2 catalysts in a solvent system with or without a base (as per Table 2, 3 and 4). The combined reaction mass was heated at the 80°C for one hour. After the completion of the reaction, the reaction product was, then, recovered with diethyl ether (5 x 2 mL) and further purified by column chromatography. Isolated ionic liquid immobilized Pd@MMT-1 clay was further dried in high vacuum at 50°C for 0.5 hours to evaporate all the volatile impurities. After the vacuum treatment, all the reactants were added as per the above-mentioned protocol with ionic liquid immobilized Pd@MMT-1 clay to recycle the catalytic system.

Ethical approval: The conducted research is not related to either human or animals use.

# 3 Results and Discussion

Task-specific [DAMI][$NTf_2$] ionic liquid was synthesized as per our previously reported procedure. We synthesized two different types of Pd@MMT clay 1 & 2, followed by mixing the neat Na-MMT clay with aqueous solution tetraamminepalladium(II) chloride monohydrate in acidic medium for 24 hours at room temperature to ensure complete exchange of palladium metal ion with the exchangeable cation of MMT clay. After the exchange, the Pd@MMT clay was washed several times deionized water and dried under lyophilizer. We obtained Pd@MMT clay-1 while mixing MMT clay with 6 mM aqueous solution of tetraamminepalladium(II) chloride monohydrate. Pd loading on MMT clay was determined by calculating the change between the concentrations of palladium metal ion in initial tetraamminepalladium(II) chloride monohydrate solution with respect to the mother liquor recovered after the filtration of Pd@MMT clay followed by inductively coupled plasma emission spectroscopy (ICP-OES). We obtained good palladium metal ion loading over Pd@MMT-1 clay (0.95% w/w Pd metal) in comparison with Pd@MMT-2 clay (0.51 % w/w Pd metal, obtained by mixing 3mM aqueous solution of tetraamminepalladium(II) chloride monohydrate with MMT clay).

The change in the basal spacing of Pd @MMT clay with respect to neat MMT clay was studied using small to medium angle X-ray scattering (SAXS) analysis (Figure 1, supporting information). In SAXS study, an increase in the basal spacing of neat MMT clay was ($d_{001}$=12.95 Å) recorded after the intercalation of palladium metal ion within the interlayer spacing of MMT clay. After the intercalation, the basal spacing of Pd@MMT-1 clay was increased up to $d_{001}$=15.86 Å. Such significant increase in $d_{001}$ spacing of MMT clay confirms the presence of palladium metal ion between the interlayer spaces of MMT clay. Sharp 001 XRD peaks gave a clear indication of parallel arrangements of clay sheets and the uniform addition of Pd NPs (Figure 2 supporting information) [13-15]. Therefore, we can conclude the presence of an ordered lamellar structure of Pd metal loaded MMT with the face-to-face arrangement of MMT clay sheets. We obtained a small characteristic signal as a peak in XRD data of Pd@MMT clay which confirms the presence of Pd NPs in MMT clay. The XRD signals of Pd NPs appeared as sharp peaks near to 40, 46 and 68 degrees respectively, representing the (111), (200) and (220) Bragg reflection. The XRD pattern of Pd metal was found in good agreement of JCPDS standard (#05-0681) and confirmed the synthesis of Pd NPs within the interlayer spacing of MMT clay. Face-centered cubic (fcc) crystal structure was used to calculate the size of Pd NPs using peak broadening profile of (111) signal at 40° using the Scherrer equation. The calculated crystallite size of the Pd NPs was found in 6.5 nm size for Pd@MMT-1 clay and 8.75 nm size for Pd@MMT-2 clay. We also studied the effect of the ionic liquid on the basal spacing of MMT clay. The sign of an increase in basal spacing of Pd@MMT -2 clay was also noticed and it was found near to $d_{001}$=14.15Å.

The morphology of MMT clay with and without Pd metal exchange and the particle size of Pd NPs as well as the presence of Pd NPs within the interlayer spacing was further confirmed by performing the high-resolution transmission electron microscopy (HRTEM) (Figure 3 supporting information). We obtained the agglomeration free uniform distribution of Pd NPs within the interlayer spacing of MMT clay. In Pd@MMT-1 clay, the particle size of Pd was recorded near to 7.5 nm with a standard deviation of ± 0.15 nm while some increase in the particle size of Pd metal was observed near to 12.5 nm with a standard deviation of ± 0.21 nm with Pd@MMT-2 clay.

During the reaction, Pd@MMT clay was used as a catalyst with functionalized ionic liquid used as a reaction medium as well as an effective substitute of amine. Presence of functionalized ionic liquid with Pd@MMT clay creates a chance of cation exchange between the cationic part of ionic liquid with remaining unexchanged $Na^+$ ions in the Pd@MMT clay (Figure 4 supporting information) [14, 15]. This type of exchange was confirmed by further SAXS analysis and FT IR analysis. The presence of characteristic bands near to 1650, 1543, 843 $cm^{-1}$ both in [DAMI][$NTf_2$] ionic liquid and $[DAMI]^+$ ion exchanged Pd@MMT clay confirmed the exchange of remaining $Na^+$ ions with cations of [DAMI][$NTf_2$] ionic liquid (Figure 5 supporting information). This exchange was also supported by SAXS analysis and $d_{001}$ spacing was reaching up to 16.76 Å from 15.86 Å in Pd@MMT-1 clay. The same change in Pd@MMT-2 clay was also recorded where the basal spacing has increased from 14.15 Å to 15.01 Å.

The textural properties of Na-MMT clay and Pd@MMT clays represented them as mesoporous solid (Table 1, Figure 6).

The nitrogen adsorption-desorption isotherm of neat MMT, Pd@MMT clay 1 and Pd@MMT clay 2 gave typical type IV with hysteresis loop at $P/P_0$ ~ 0.4 to 0.9 (Figure 6 supporting information). This data reveals no change in the porous structure of Na-MMT clay even after the insertion of Pd NPs. A drop in the BET surface area and total pore volume after the intercalation Pd NPs was recorded mainly due to the capping of some pores with metal NPs. The data shows the development of adsorbent multipliers' and weak adsorbate-adsorbent connections. The different shapes of the adsorption-desorption isotherms were due to the configuration and size distribution of Pd NPS. Absenteeism of any unexpected changes in the surface area and pore volume supported the no sign of agglomeration.

Energy dispersive X-ray spectroscopy (EDS) was applied to understand the chemical composition of Pd@MMT clay to better know the structure and homogeneity of prepared materials (Figure 7 supporting information). The presence of characteristic signals of Pd metal in EDS spectra confirmed the presence of Pd NPs. The XPS analysis of Pd metal in Pd@MMT clays gave two characteristic peaks for Pd $3d_{5/2}$ and $3d_{3/2}$ at 335.3 eV and 340.5 eV respectively (Figure 7 supporting information). This data confirmed the presence of well reduced Pd (0) NPs within the interlayer spacing of MMT clay. Heterogeneous nature of catalysts was examined by catalyst poising experiment (supporting information).

After the completion of the careful physiochemical analysis of Pd-MMT clay, we further used them as a catalyst for two very important reactions usingthe Mizoroki-Heck reaction.

## 3.1 Mizoroki-Heck Reaction with Pd@MMT Clay as Catalyst

Alkenylphosphonates are considered an important chemical in medical science, material science and as polymer additives [18]. Various protocols such as the Suzuki - Miyaura coupling of boronic acids with vinylphosphonate, a Mizoroki-Heck reaction using vinylphosphonate with different aryl derivatives, aldehyde insertion into zirconacycle phosphonates and Olefin cross-metathesis have been reported using numerous transition metal catalytic systems under a toxic conventional solvent

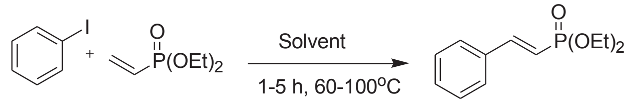

**Scheme 1:** Model Mizoroki- Heck reaction.

**Table 1:** Surface properties of Na-MMT clay and Pd@MMT clays.

| Samples | BET surface area (m$^2$/g) | Average Pore size (nm) | Pore volume (cm$^3$/g) |
|---|---|---|---|
| Na-MMT | 385 | 3.48 | 0.362 |
| Pd@MMT clay-1 | 371 | 3.32 | 0.211 |
| Pd@MMT clay-2 | 379 | 3.39 | 0.209 |

system [18-22]. The reaction is primarily suffering from catalyst recycling and the requirement of the toxic base for the successful completion of the reaction. In this report, we are using our well characterized Pd@MMT clay catalysts to improve the reaction kinetics of vinyl phosphonates synthesis followed by Mizoroki -Heck reaction. Also, we are exploring the synthesis of a unique double-Mizoroki-Heck reaction using our developed MMT supported Pd catalytic system.

Initially, we allowed Pd @MMT clay 1 to catalyze a model Mizoroki- Heck reaction between iodobenzene and diethyl vinyl phosphonate under functionalized ionic liquid medium (instead of using the toxic conventional solvent system and toxic base) at 80°C for 1 hour (Scheme 1, Table 2). We successfully obtained the

**Table 2:** Reaction optimization of Mizoroki Heck reaction.

| Entry | Catalyst (0.01 g) | Solvlnent (0.150 g) | Base (1 mmol) | Time (h) | Temperature (°C) | Yield (%) |
|---|---|---|---|---|---|---|
| 1. | Pd@MMT clay-1 | [DAMI][NTf$_2$] | - | 1 | 80 | 92 |
| 2. | Pd@MMT clay-2 | [DAMI][NTf$_2$] | - | 1 | 80 | 55 |
| 3. | Pd@MMT clay-1 (0.02g) | [DAMI][NTf$_2$] | - | 1 | 80 | 92 |
| 4. | Pd@MMT clay-1 (0.005g) | [DAMI][NTf$_2$] | - | 1 | 80 | 52 |
| 5. | Pd@MMT clay-1 | [DAMI][NTf$_2$] (0.200 g) | - | 1 | 80 | 91 |
| 6. | Pd@MMT clay-1 | [DAMI][NTf$_2$] (0.100 g) | - | 1 | 80 | 72 |
| 7. | Pd@MMT clay-1 | [DAMI][NTf$_2$] | KOH | 1 | 80 | 90 |
| 8. | Pd@MMT clay-1 | [DAMI][NTf$_2$] | $K_2CO_3$ | 1 | 80 | 87 |
| 9. | Pd@MMT clay-1 | [DAMI][NTf$_2$] | $^{i}Pr_2NH$ | 1 | 80 | 91 |
| 10. | Pd@MMT clay-1 | [DAMI][NTf$_2$] | $Et_3N$ | 1 | 80 | 90 |
| 11. | Pd@MMT clay-1 | [bmim][NTf$_2$] |  | 1 | 80 | 35 |
| 12. | Pd@MMT clay-1 | [bmim][NTf$_2$] | $^{i}Pr_2NH$ | 1 | 80 | 73 |
| 13. | Pd@MMT clay-1 | [DAMI][NTf$_2$] | - | 1 | 50 | 34 |
| 14. | Pd@MMT clay-1 | [DAMI][NTf$_2$] | - | 1 | 100 | 91 |
| 15. | Pd@MMT clay-1 | [DAMI][NTf$_2$] | - | 2 | 100 | 91 |
| 16. | Pd@MMT clay-1 | [DAMI][NTf$_2$] | - | 30 | 100 | 42 |
| 17. | Pd@MMT clay-1 | DMF | $^{i}Pr_2NH$ | 1 | 80 | 66 |
| 18. | Pd@MMT clay-1 | THF | $^{i}Pr_2NH$ | 1 | 80 | 59 |
| 19. | Pd@MMT clay-1 | $CH_3CN$ | $^{i}Pr_2NH$ | 1 | 80 | 45 |
| 20. | $Pd(NH_3)_4Cl_2{\cdot}H_2O$ | [DAMI][NTf$_2$] | - | 1 | 80 | 65 |
| 21. | $Pd(OAc)_2$ | [DAMI][NTf$_2$] | - | 1 | 80 | 61 |
| 22. |  | [DAMI][NTf$_2$] | - | 1 | 80 | - |

corresponding reaction product with good yield. The same reaction condition was also tested with Pd@MMT clay-2 catalyst unfortunately, lower yield was recorded due to low Pd metal loading (Table 2, entry 2).

No sign of drastic change in the yield of Mizoroki-Heck reaction was observed when elevating the reaction temperature or time and quantity of ionic liquid or catalyst. But, as expected, while lowering the reaction condition, a clear drop in reaction yield was recorded. Replacement of functionalized ionic liquid with a series of base and non- functionalized [bmim][NTf$_2$] ionic liquid showed the importance of [DAMI][NTf$_2$] ionic liquid which works as active bases (due to the presence of two -NH functional group) and effective reaction medium. We also received lower catalytic activity of conventional Pd catalysts over our developed Pd@MMT clay catalytic system in ionic liquid medium (Table 2, entry 20 and 21). No sign of reaction product was recorded in absence of Pd@MMT clay 1 catalyst. After reaction completion, the product was effortlessly isolated *via* diethyl ether extraction and further purified using column chromatography. We successfully recycled our ionic liquid immobilized Pd@MMT-1 clay up 8 cycles without showing any significant loss in catalytic activity in terms of reaction yield. Surprisingly, no signature of catalyst leaching was recorded while performing a filtration test during recycling experiments. All the solid material was isolated with 0.45 mm polytetrafluoroethylene (PTFE) filter and recovered liquid was mixed with the reactants of the model Mizoroki heck reaction. No product formation was recorded during this reaction which confirmed the zero leaching of Pd metal from MMT clay. These filtration experiments were also supported by ICP-OES analysis of above-mentioned filtrate, where no signal from Pd metal was received. A sign of agglomeration and low reaction yield was recorded in TEM image analysis after 8 times recycling of Pd@MMT clay-1 catalyst (Figure 3 and 8 supporting information). Due to agglomeration, particle size increase in Pd NPs was observed from 7.5 nm to 19.5 nm (with a standard deviation of ± 0.75 nm). In some of the reports, the formation of palladium black was reported due to high reaction temperature [1-3]. In our case, no such observation was found mainly due to the extended thermal stability of Pd NPs because of thermally stable MMT clay.

We applied the optimized reaction conditions for the variance of aryl halides and with different types of dialkylvinylphophonates. All the results were summarized Table 3, Scheme 2.

We tested a variety of aryl iodide (electron rich and electron poor) with two different types of vinyl

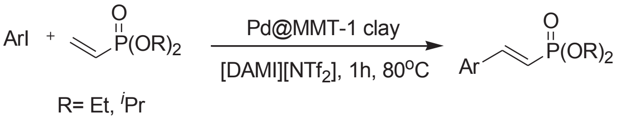

**Scheme 2:** Mono Mizoroki-Heck reaction.

**Table 3:** Pd@MMT-1 clay catalyzed mono Mizoroki-Heck reaction.

| Entry | Aryl halide (1mmol) | Phosphonate (2 mmol) | Yield (%) |
|---|---|---|---|
| 1. | 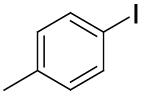 | 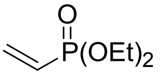 | 89 |
| 2. | | 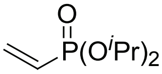 | 83 |
| 3. | 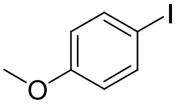 | 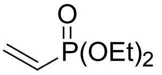 | 86 |
| 4. | | 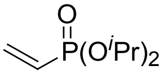 | 81 |
| 5. | 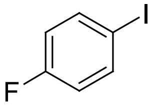 | 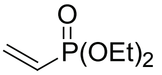 | 92 |
| 6. | | 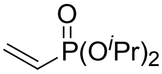 | 91 |
| 7. | 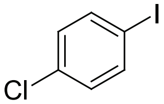 | 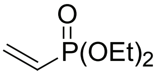 | 91 |
| 8. | | 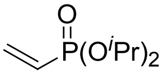 | 93 |
| 9. | 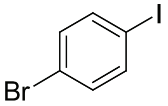 | 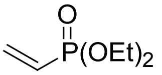 | 84 |
| 10. | | 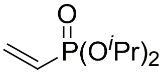 | 86 |
| 11. | 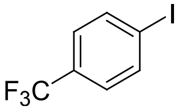 | 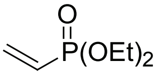 | 87 |
| 12. | | 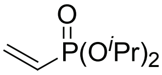 | 91 |
| 13. | 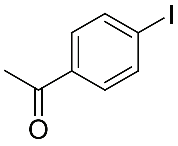 | 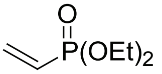 | 92 |
| 14. | | 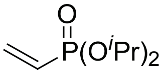 | 91 |
| 15. | 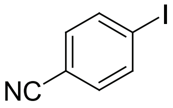 | 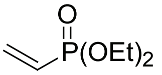 | 86 |
| 16. | | 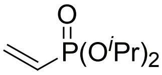 | 88 |

Continued **Table 3:** Pd@MMT-1 clay catalyzed mono Mizoroki-Heck reaction.

| Entry | Aryl halide (1mmol) | Phosphonate (2 mmol) | Yield (%) |
|---|---|---|---|
| 17. | 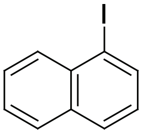 | 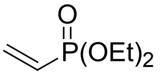 | 85 |
| 18. | | 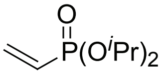 | 83 |
| 19. | 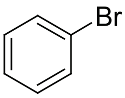 | 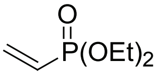 | 66 |
| 20. | | 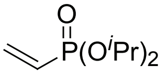 | 67 |
| 21. | 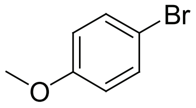 | 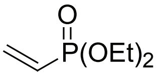 | 59 |
| 22. | | 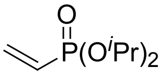 | 55 |
| 23. | 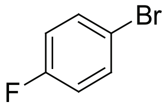 | 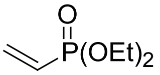 | 70 |
| 24. | | 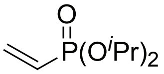 | 69 |
| 25. | 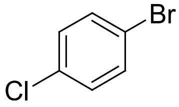 | 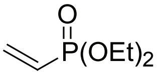 | 70 |
| 26. | | 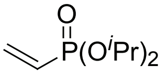 | 76 |
| 27. | 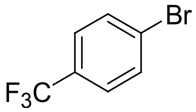 | 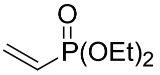 | 76 |
| 28, | | 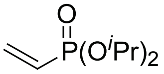 | 77 |
| 29., | 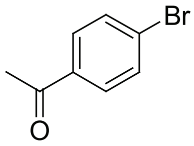 | 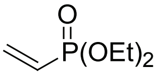 | 73 |
| 30. | | 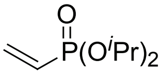 | 80 |
| 31. | 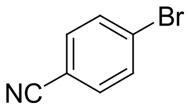 | 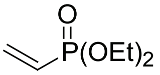 | 74 |
| 32. | | 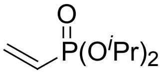 | 75 |
| 33. | 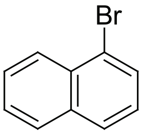 | 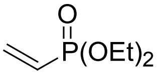 | 62 |
| 34. | | 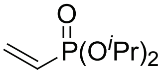 | 63 |

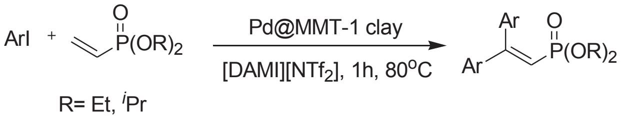

**Scheme 3:** Double Mizoroki-Heck reaction.

phosphonate derivatives. We obtained good to excellent yield in all cases. Surprisingly, lowering of reaction yield was not reported with sterically hindered aryl halides (Table 3, entry 15-18). We easily performed typical oxidative addition of aryl bromide derivatives with MMT supported Pd metal without increasing the reaction temperature, reaction time and catalyst loading (Table 3, entry 19-30). This outcome represented the high catalytic performance of Pd@MMT -1 clay catalyst in the ionic liquid medium. We obtain the slow reaction rate with electron-rich aryl bromide derivatives than electron deficient composition. The presence of steric effect on aryl bromide derivatives as low reaction yield was recorded in their corresponding reaction products (Table 3, entry 31-34.).

### 3.2 Double Mizoroki-Heck Reaction

In our study, we also extended the application of Pd@ MMT-1 clay catalysts for double-Mizoroki-Heck reaction while changing the limiting reagent from aryl halides to vinyl phosphonates (Scheme 3, Table 4, Entry 1-14). We obtained the corresponding double-Mizoroki-Heck reaction products with average to good yield. A series of electron rich and electron poor aryl halides were easily converted to their reaction products (Table 4, Entry 1-10).

Sterically hindered aryl iodides were easily converted to 2, 2,-diary vinyl phosphonates with good yields (Table 4, entry 11-12). This result confirmed no effect of steric hindrance on double Mizoroki-Heck reaction. In addition, brominated aryl halides were allowed to react with vinyl phosphonates without changing any reaction condition *via* double Mizoroki-Heck reaction and their matching reaction products were nicely isolated in good yield.

## 4 Conclusions

The cation exchanged method was used to prepare two different types of Pd@MMT clays with different Pd loading. All the catalysts were properly analyzed through advanced analytical techniques including FTIR, ICP-OES, SAXS, XRD, FTIR, $N_2$ physisorption, EDS and TEM. High Pd NP

**Table 4:** Pd@MMT-1 clay catalyzed double Mizoroki-Heck reaction.

| Entry | Aryl halide (2 mmol) | Phosphonate (1 mmol) | Yield (%) |
|---|---|---|---|
| 1. | 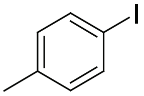 | 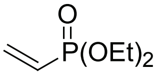 | 72 |
| 2. | | 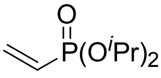 | 66 |
| 3. | 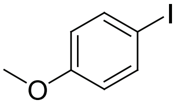 | 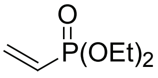 | 69 |
| 4. | | 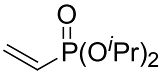 | 64 |
| 5. | 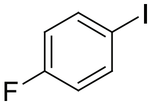 | 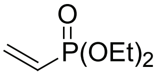 | 75 |
| 6. | | 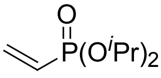 | 74 |
| 7. | 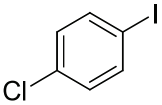 | 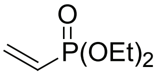 | 74 |
| 8. | | 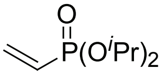 | 76 |
| 9. | 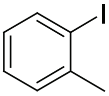 | 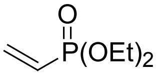 | 70 |
| 10. | | 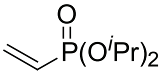 | 74 |
| 11. | 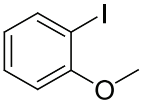 | 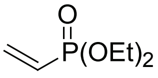 | 75 |
| 12. | | 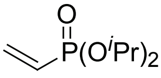 | 74 |
| 13. | 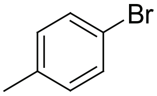 | 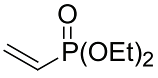 | 75 |
| 14. | | 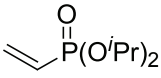 | 74 |
| 15. | 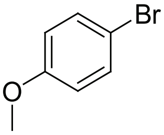 | 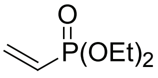 | 75 |
| 16. | | 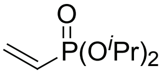 | 74 |

loading, agglomeration free, narrow size distributed Pd NPs were reported in Pd@MMT-1 clay over Pd@MMT-2 clay. A high degree of mesoporous nature was also calculated in Pd@MMT-1 clay. Here, we also prepared two types of functional and nonfunctional ionic liquids to use them as an active solvent system in our reaction. In our report, we also investigated the benefits ionic liquids, other than reaction medium, and concluded that the exchange of ionic liquid cations with the remaining $Na^+$ cations of Pd@MMT clay has expanded the interlayer spacing to accommodate better reaction between Pd NPs and reactants. Such feature of ionic liquid found responsible for the highly selective Mizoroki-Heck reaction. Pd@MMT clay under catalyst recycling experiments was found highly active under thermal heating and successfully recycled the Pd@MMT-1 clay catalyst up to 8 runs. Surprisingly, no catalysts leaching was recorded during catalysts recycling experiments. Along with mono Mizoroki-Heck reaction, we also obtained double Mizoroki-Heck reaction with a good reaction yield without increasing reaction time/temperature and catalyst loading. In addition, we developed an operationally simple catalytic recycling system for Mizoroski-Heck reaction without using any toxic ligands and harmful conventional solvent systems.

Conflict of interest: Authors state no conflict of interest.

## References

[1] Pagliaro M., Pandarus V., Ciriminna R., Béland F., Demma Carà P., Heterogeneous versus homogeneous palladium catalysts for cross-coupling reactions, ChemCatChem, 2012, 4(4), 432-445.

[2] Karimi B., Mansouri F., Mirzaei H.M., Recent applications of magnetically recoverable nanocatalysts in C-C and C-X coupling reactions, ChemCatChem, 2015, 7(12), 1736-1789.

[3] Dong Z., Ye Z., Reusable, highly active heterogeneous palladium catalyst by convenient self-encapsulation cross-linking polymerization for multiple carbon-carbon cross-coupling reactions at ppm to ppb palladium loadings, Adv. Synth. Catal., 2014, 356(16), 3401-3414.

[4] Upadhyay P.R., Srivastava V., Recyclable graphene-supported palladium nanocomposites for Suzuki coupling reaction, Green Process, Synth., 2016, 5, 123-129.

[5] Balanta A., Godard C., Claver C., Pd nanoparticles for C-C coupling reactions, Chem. Soc. Rev., 2011, 40(10), 4973-4985.

[6] Kumar B.S., Anbarasan R., Amali A.J., Pitchumani K., Isolable C@$Fe_3O_4$ nanospheres supported cubical Pd nanoparticles as reusable catalysts for stille and mizoroki-Heck coupling reactions, Tetrahedron Lett., 2017, 58(33), 3276-3282.

[7] Taladriz-Blanco P., Hervés P., Pérez-Juste J., Supported Pd nanoparticles for carbon–carbon coupling reactions, Top. Catal., 2013, 56(13), 1154-1170.

[8] Phan N.T.S., Van Der Sluys M., Jones C.W., On the nature of the active species in palladium catalyzed mizoroki–Heck and suzuki–miyaura couplings – homogeneous or heterogeneous catalysis, A critical review, Adv. Synth. Catal., 2006, 348(6), 609-679.

[9] Chen S.-Y., Attanatho L., Mochizuki T., Zheng Q., Toba M., Yoshimura Y., Somwongsa P., Lao-Ubol S., Influences of the support property and Pd loading on activity of mesoporous

silica-supported Pd catalysts in partial hydrogenation of palm biodiesel fuel, Adv. Porous Mater., 2016, 4(3), 230-237.

[10] Wang J., Li Y., Li P., Song G., Polymerized functional ionic liquid supported Pd nanoparticle catalyst for reductive homocoupling of aryl halides, Monatshefte für Chemie - Chemical Monthly, 2013, 144(8), 1159-1163.

[11] Yamada Y.M.A., Takeda K., Takahashi H., Ikegami S., An assembled complex of palladium and non-cross-linked amphiphilic polymer: A highly active and recyclable catalyst for the suzuki–miyaura reaction, Org. Lett., 2002, 4(20), 3371-3374.

[12] Li X., Zhou F., Wang A., Wang L., Wang Y., Hydrodesulfurization of dibenzothiophene over MCM-41-supported Pd and Pt catalysts, Energy Fuels, 2012, 26(8), 4671-4679.

[13] Upadhyay P.R., Srivastava V., Clays: An encouraging catalytic support, Curr. Catal., 2016, 5(3), 162-181.

[14] Srivastava V., Ru-exchanged MMT clay with functionalized ionic liquid for selective hydrogenation of $CO_2$ to formic acid, Catal. Lett., 2014, 144(12), 2221-2226.

[15] Upadhyay P., Srivastava V., Ruthenium nanoparticle-intercalated montmorillonite clay for solvent-free alkene hydrogenation reaction, RSC Adv., 2015, 5(1), 740-745.

[16] Patil M.R., Kapdi A.R., A V.K., A recyclable supramolecular-ruthenium catalyst for the selective aerobic oxidation of alcohols on water: Application to total synthesis of Brittonin A, ACS Sustainable Chem. Eng., 2018.

[17] Upadhyay P.R., Srivastava V., Selective hydrogenation of $CO_2$ gas to formic acid over nanostructured Ru-$TiO_2$ catalysts, RSC Adv., 2016, 6(48), 42297-42306.

[18] Nagaoka Y., Carbon-carbon bond formation based on alkenylphosphonates, Yakugaku Zasshi, 2001, 121(11), 771-779.

[19] Baird L.J., Colomban C., Turner C., Teesdale-Spittle P.H., Harvey J.E., Alkenylphosphonates: Unexpected products from reactions of methyl 2-[(diethoxyphosphoryl)methyl]benzoate under Horner-Wadsworth-Emmons conditions, Org. Biomol. Chem., 2011, 9(12), 4432-4435.

[20] Lee S.Y., Lee B.S., Lee C.-W., Oh D.Y., Synthesis of 4-oxo-2-alkenylphosphonates via nitrile oxide cycloaddition: γ-Acylation of allylic phosphonates, J. Org. Chem., 2000, 65(1), 256-257.

[21] Kabalka G.W., Guchhait S.K., Synthesis of (E)- and (Z)-alkenylphosphonates using vinylboronates, Org. Lett., 2003, 5(5), 729-731.

[22] Vinokurov N., Michrowska A. Szmigielska A., Drzazga Z., Wójciuk G., Demchuk O.M., Grela K., Pietrusiewicz K.M., Butenschön H., Homo- and cross-olefin metathesis coupling of vinylphosphane oxides and electron-poor alkenes: Access to P-stereogenic dienophiles, Adv. Synth. Catal., 2006, 348(7-8), 931-938.